A Historical Perspective of the La Niña in 2020-21

Zeng-Zhen Hu (Xiaofan Li, Yu-heng Tseng, Yunyun Liu, and Ping Liang)

Climate Prediction Center, NCEP/NWS/NOAA, MD 20740, USA

Main Results

- ❖ **2020/21 La Niña was uniquely preceded by a borderline El Niño instead of an El Niño.**
- ❖ **Compared with other strong La Niña events, the anomalies extended further eastward in 2020/21 La Niña.**
- ❖ **The strength of all the strong La Niña events is determined by the in-phase amplification of all time scale variations. Their decay in the boreal spring and early summer is mainly controlled by the intraseasonal-interseasonal variation.**
- ❖ **2020/21 La Niña was successfully predicted, however, the North American climate anomalies didn't match the typical La Niña response.**

1: Questions

Q1: What are the differences of 2020/21 La Nina compared with the historical strong La Niña events?

Q2: What are the contributions of different time scale components to the strength and evolution of the strong La Niña events since 1982?

Q3: What are the real-time predictions of the La Niña events from a climate model and the unexpected impact on the North American climate?

2: Model and Methods

The ocean temperature data are from GODAS (Behringer 2007). The Kelvin wave index is defined as standardized projections of GODAS ocean temperatures onto the first mode of an extended EOF (Seo and Xue 2005). The warm water volume (WWV) index is defined as the D20 anomaly averaged in (5ºS-5ºN, 120ºE-80ºW) (Meine and McPhaden 2000).

SST is from OIv2 SST (Reynolds et al., 2002). ENSO is defined based on both the Niño3.4 index and the relative Niño3.4 index. The Niño3.4 index is the SSTA averaged in (5°S−5°N, 170°W−120°W), while the relative Niño3.4 index is the Niño3.4 index minus the SSTA averaged in the whole tropics (0°-360°, 20°S-20°N; van Oldenborgh et al. 2021). The relative Niño3.4 index is renormalized by multiplying by 1/(1−A) with "A" the regression of the 20°S–20°N SSTAs on the Niño3.4 index.

Atmospheric data are from NCEP R2 (Kanamitsu et al. 2002), OLR from Liebmann and Smith (1996), and observation-based precipitation analysis from CMAP (Xie and Arkin 1997). Except for the OIv2 SST data from Nov. 1981 to Dec. 2021, all other observational-based data used in this work are from Jan. 1979 to Dec. 2021. All the anomalies are referred to as the departures from climatologies during Jan. 1991–Dec. 2020.

To identify the contributions of different time scales to the intensity and evolution of various strong La Niña events, Ensemble Empirical Mode Decomposition (EEMD) is adopted (Wu and Huang 2009).

The real-time predictions of the La Niña in 2020/21 with ICs of Jan. 2020-May 2021 and precipitation in Dec. 2020-Feb 2021 are from the NCEP CFSv2 (Xue et al., 2013; Saha et al., 2014). The 9-month predictions include 80 members within the last 20 days of each month and four forecasts per day with ICs from CFSR (Saha et al. 2010; Xue et al. 2011).

3: SUMMARY

- ➢ 2020/21 La Niña emerged in August 2020 and dissipated in May 2021.
- ➢ 2020/21 La Niña was uniquely preceded by a borderline El Niño instead of an El Niño and a weak equatorial-heat discharge process. That resulted in the weakest event among the strong La Niñas since 1982, although there were strong upwelling Kelvin wave activities.
- ➢ Compared with other strong La Niña events, the surface easterly wind anomalies and the warm pool extended further eastward in 2020/21 La Niña, linking to a relatively weaker dipole-like pattern of the subsurface ocean temperature anomalies.
- ➢ The strength of all the strong La Niña events is determined by the in-phase amplification of all time scale variations. Their decay in the boreal spring and early summer is mainly controlled by the intraseasonal-interseasonal variation.
- ➢ 2020/21 La Niña was successfully predicted, however, the North American climate anomalies didn't match the typical La Niña response.

4: A Historical Perspective of 2020/21 La Niña

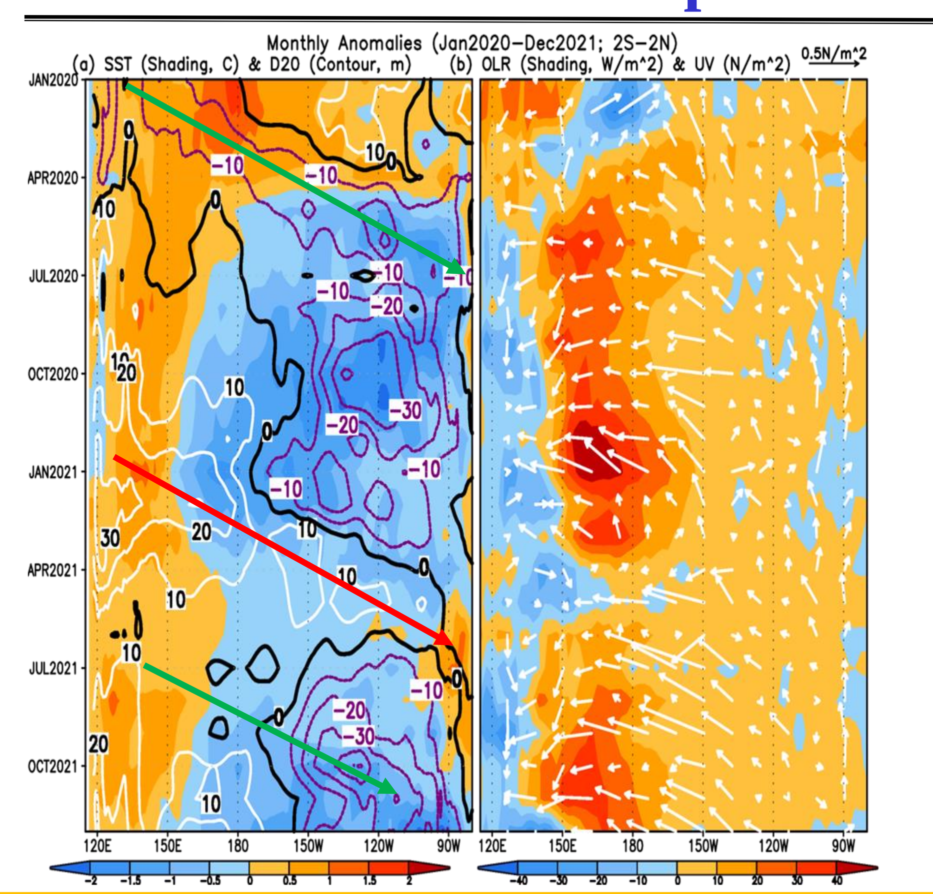

- ➢ The negative SSTAs were initiated in Apr 2020 and accompanied by a strong upwelling Kelvin wave represented by negative D20As.
- ➢ The negative SSTAs weakened slightly in Jun 2020 after the upwelling Kelvin wave reached the South American coast. Then, the negative SSTAs re-strengthened and reached their peak in Oct-Dec 2020.
- ➢ In consistence with the SSTA pattern (warming in the western & cooling in the eastern equatorial Pacific), convection was suppressed in the central tropical Pacific, and low-level easterly wind anomalies prevailed in the equatorial Pacific since Jul 2020.

Fig. 1: Hovmöller diagrams of the monthly mean of (a) SST (shading) and D20 (contours) anomalies, and (b) OLR (shading) and surface wind stress (vector) anomalies averaged in 2^{o}S-2^{o}N during (a) Jan 2020-Dec 2021. The units are ^{o}C for SST, m for D20, W/m2 for OLR, and N/m2 for wind stress.

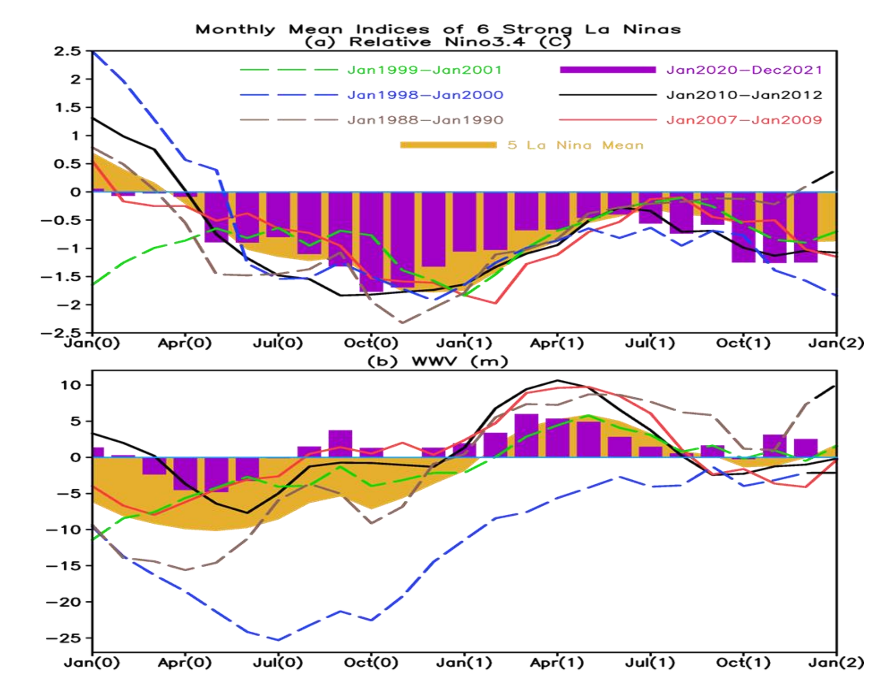

- ➢ The La Niña event imitated in May 2020 and ended in May 2021.
- ➢ Historically, there are six-strong La Niña events with the peak values of the relative Niño3.4 index ≤ - 1.5^{o}C during 1982-2021: 1988/89, 1998/99, 1999/2000, 2007/08, 2010/11, and 2020/21. The peak values of the relative Niño3.4 index are -2.32^{o}C in Nov 1988, -1.93^{o}C in Dec 1998, -1.84^{o}C in Jan 2000, -1.98^{o}C in Feb 2008, -1.84^{o}C in Sep 2010, and -1.77^{o}C in Oct 2020, respectively.
- ➢ From the historical perspective, 2020/21 La Niña ranks 6th in the strength based on the monthly mean relative Niño3.4 index and is the weakest strong La Niña event (weakest WWV) since 1982.

Fig. 2: Time evolution of the monthly mean (a) relative Niño3.4 and (b) WWV indices during six-strong La Niña events: Jan 1988-Jan 1990 (brown dash line), Jan 1998-Jan 2000 (blue dash line), Jan 1999-Jan 2001 (green dash line), Jan 2007-Jan 2009 (red solid line), Jan 2010-Jan 2012 (black solid line), and Jan 2020-Dec 2021 (purple bars). The shading represents the average of the first five events. The unit is ^{o}C for (a) and m for (b).

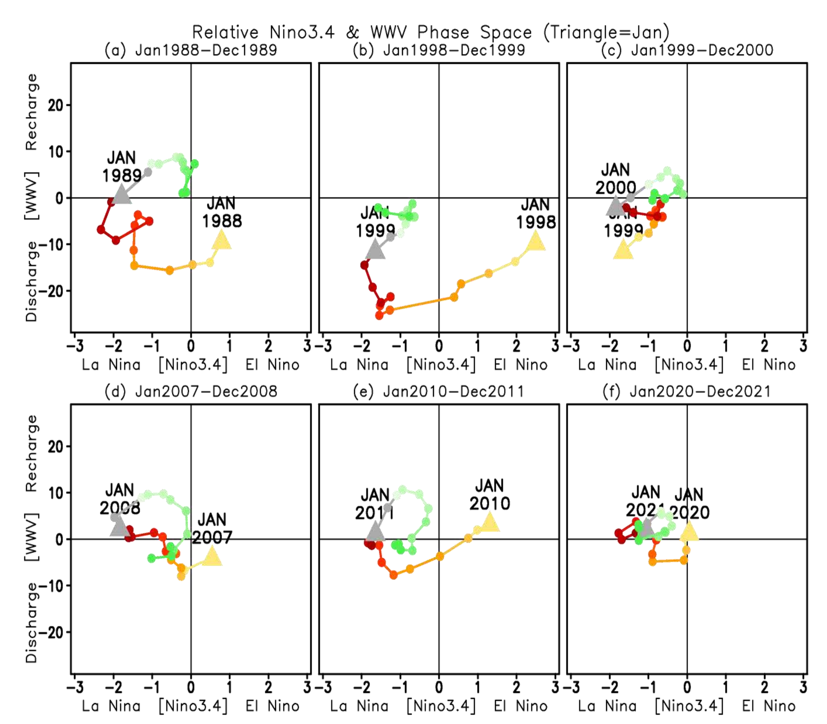

- ➢ Compared with other strong La Nina years, both the recharge/discharge are weaker during 2020/21.

Fig. 3: Phase orbits of the monthly mean relative Niño3.4 (x-axis; °C) and WWV (y-axis; m) indices during (a) Jan 1988-Dec 1989, (b) Jan 1998-Dec 1999, (c) Jan 1999-Dec 2000, (d) Jan 2007-Dec 2008, (e) Jan 2010-Dec 2011, and (f) Jan 2020-Dec 2021. The triangle marks represent January and different colors represent different months.

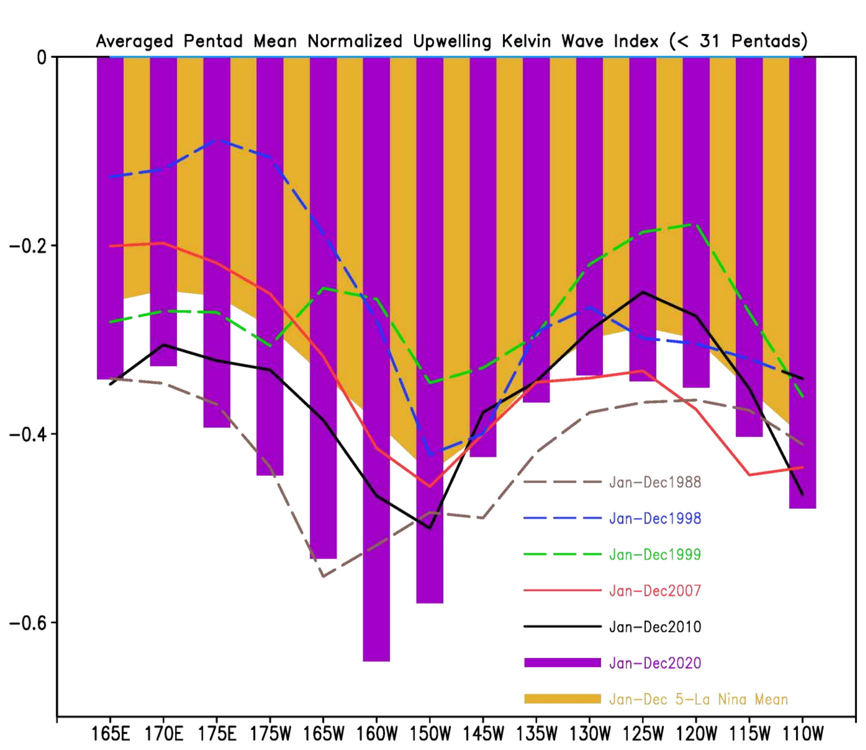

- ➢ 2020/21 La Niña was uniquely followed by a borderline El Niño instead of an El Niño, the equatorial-heat discharge was the weakest among the strong La Niñas since 1982.
- ➢ However, the overall upwelling Kelvin wave was relatively strong during its development phase, leading to a weakest strong event.

Fig. 4: Longitude−dependent negative pentad oceanic Kelvin wave index averaged in Jan-Dec during the development years of the six-strong La Niña events: 1988 (brown dash line), 1998 (blue dash line), 1999 (green dash line), 2007 (red solid line), 2010 (black solid line), and 2020 (purple bars). The shading represents the average of the first five events. To eliminate the stationary component, the 31-pentad running mean is removed.

5: Contribution of different time scale variations to the strength and evolution of the strong La Niñas

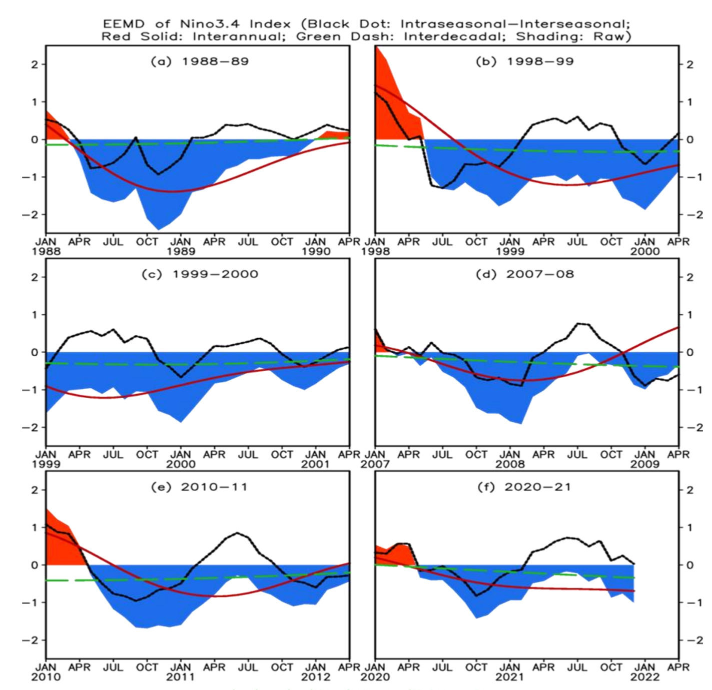

- ➢ The strength of all the strong La Niña events is determined by the in-phase amplification of all time scale variations.
- ➢ Their decay in the boreal spring and early summer is mainly controlled by the intraseasonal-interseasonal variation.

Fig. 5: Monthly mean Niño3.4 index during (a) Jan 1988-Apr 1990, (b) Jan 1998-Apr 2000, (c) Jan 1999-Apr 2001, (d) Jan 2007-Apr 2009, (e) Jan 2010-Apr 2012, and (f) Jan 2020-May 2021. The shading, black dot, red solid, and green dash lines represent raw data, EEMD components at intraseasonal-interseasonal, interannual, and interdecadal and longer time scales, respectively. The unit is ^{o}C.

6: Predictions and the Impacts

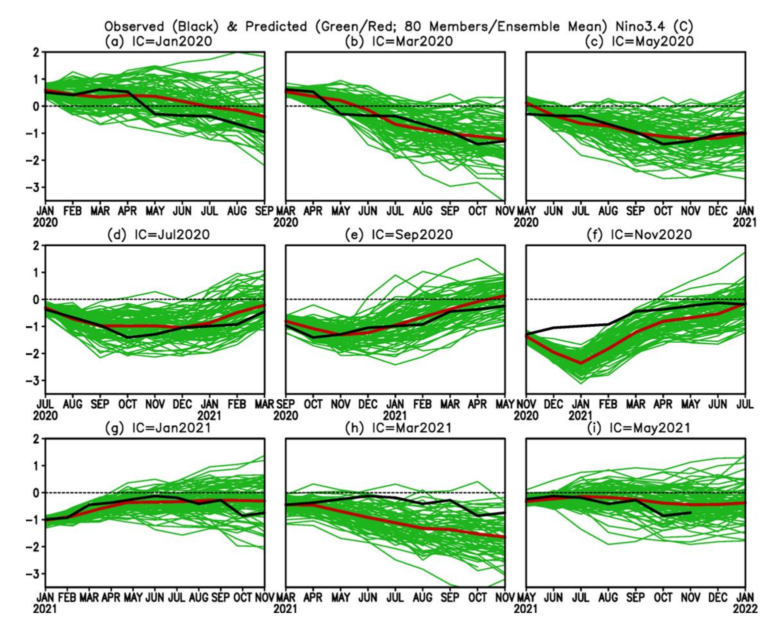

- ➢ The La Niña event in 2020/21 was successfully predicted by CFSv2 with ICs from Jan to Sep 2020, despite some biases in predicting the cooling strength.

Fig. 6: Observed (black line) and CFSv2 predicted monthly mean Niño3.4 index with initial conditions in (a) Jan 2020, (b) Mar 2020, (c) May 2020, (d) Jul 2020, (e) Sep 2020, (f) Nov 2020, (g) Jan 2021, (h) Mar 2021, and (i) May 2021. The green lines denote the 80 individual members, and the red line represents the ensemble mean of 80 members. The unit is ^{o}C.

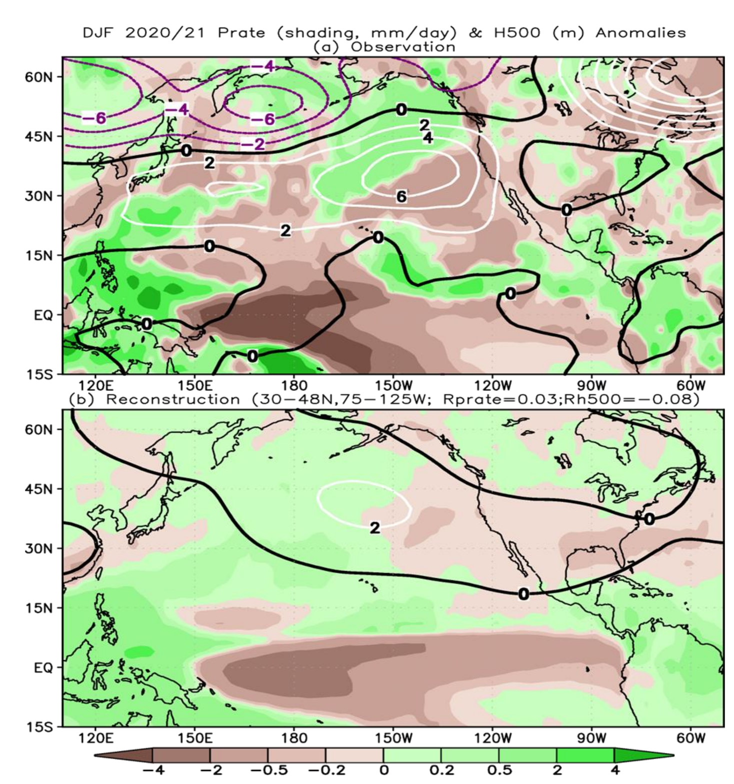

- ➢ Both the reconstructed circulation & precipitation anomalies based on the observed Niño3.4 index in DJF 2020/21 are much weaker than the observed ones.
- ➢ Moreover, consistent with Dr. Johnson's argument ((https://www.climate.gov/news-features/blogs/enso/did-northern-hemisphere-get-memo-years-la-ni%C3%B1a), there are few similarities for the spatial distribution of both the precipitation & H500 anomalies over the North American sector.

Fig. 7: Observed (a) and reconstructed (b) H500 (contours; m) and precipitation (shading; mm/day) anomalies in DJF 2020/21. The reconstructions are based on the regression onto the Niño3.4 index. The pattern correlations between the observations and the reconstruction are 0.03 for precipitation and -0.08 for H500 over the U. S. (30^{o}-48^{o}N, 75^{o}-125^{o}W).

Contact Information: **E-mail: Zeng-Zhen.Hu@noaa.gov**

Reference: Li, X., Z.-Z. Hu, Y.-h. Tseng, Y. Liu, and P. Liang: 2022: A Historical Perspective of the La Niña Event in 2020/21. J. Geophys. Res., 127 (7), e2021JD035546. DOI: 10.1029/2021JD035546.